Enhanced diffractogram improves robustness and accuracy of determination of contrast transfer function of transmission electron microscope

S. Jonić[1], C.O.S. Sorzano[2,3], R. Nuñez[2], J.M. Carazo[2], N. Boisset[1]

[1]Institut de Minéralogie et de Physique des Milieux Condensés (IMPMC), Université P et M Curie, UMR 7590, CNRS, 140 rue de Lourmel, 75015 Paris, France
[2]Unidad de Biocomputación, Centro Nacional de Biotecnología (CSIC), Campus Universidad Autónoma s/n, 28049 Cantoblanco, Madrid, Spain
[3]Dept. Ingeniería de Sistemas Electrónicos y de Telecomunicación, Univ. San Pablo-CEU, Campus Urb. Montepríncipe s/n, 28668 Boadilla del Monte, Madrid, Spain

Abstract

In a previous work, we developed a method for improving the visibility of diffraction rings of cryo-electron micrographs of vitreous ice (without carbon film or high concentration of diffracting material) [1]. We used these enhanced power spectrum densities (enhanced PSDs) to semi-automatically detect and remove micrographs and/or local areas that do not improve the global signal-to-noise ratio (*e.g.*, non-diffracting micrographs or their areas) or those that introduce errors in the global 3D map (*e.g.*, drifted micrographs or charged areas). This sorting is based on the normalized cross-correlation (NCC) between enhanced PSDs and their copies rotated by 90° [1]. In the present work, we propose to use enhanced PSDs to improve robustness and accuracy of estimation of the contrast transfer function (CTF) on images that are kept after sorting. We show that the use of enhanced PSDs can improve estimation of the PSD model proposed by Velazquez-Muriel *et al*. [2]. This method estimates a full two-dimensional PSD model including the envelope. Determination of defocus parameters (maximum defocus, minimum defocus, angle of astigmatism) is the most difficult part of PSD estimation. This is why the algorithm first estimates roughly as many parameters of the PSD model as possible (*i.e*., background and envelope parameters), and then, estimates very accurately defocus parameters based on a weighted correlation between the enhanced experimental PSD and the CTF model. In a final step, all the parameters are refined. Our algorithm is implemented in the Xmipp (open-source image processing package) and can be implemented in any other software package.

1. Improvement of visibility of diffraction rings

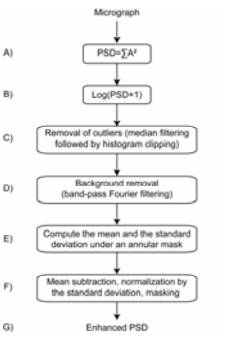

Examples of application of the enhancement algorithm (left) on two cryo-EM images without carbon film (JEOL JEM 2100F, ultra high-resolution pole piece, no tilt, voltage: 200 kV, Cs: 0.5 mm, magnification: X50.000, defocus: from -1.7 to -3.2 µm, pixel size: 1.59 Å × 1.59 Å)

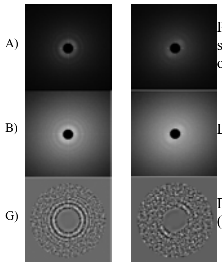

Isotropic Anisotropic

A) PSD=∑A² (Diffractogram: averaging of spectra of about 1000 overlapped sub-areas of size 512 × 512 pixels)

B) Log(PSD+1)

G) Diffractogram of an improved visibility (Enhanced PSD)

2. Sorting 151 micrographs based on sorting of their enhanced global diffractograms

Sorting based on normalized cross-correlation (NCC) between the enhanced PSDs and their copies rotated by 90°

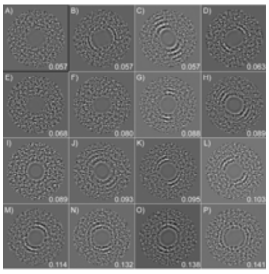

Sixteen lowest NCC values: Drifted (B-D,G-M) , non-diffracting (A,E,F), and strongly astigmatic (N-P) images.

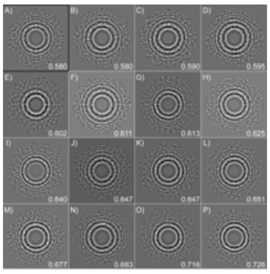

Sixteen highest NCC values: Isotropic images

3. Power spectrum density (PSD) model

PSD: $PSD_{theoretical}(\boldsymbol{\varpi}) = K^2|H(\boldsymbol{\varpi})|^2 + S_N(\boldsymbol{\varpi})$

CTF: $H(\boldsymbol{\varpi}) = -E_{\Theta_{1,2,3}}(\boldsymbol{\varpi})(\sin(\chi_{\Theta_{1,2}}(\boldsymbol{\varpi})) + Q_0\cos(\chi_{\Theta_{1,2}}(\boldsymbol{\varpi})))$

$\Theta_1 = (V, C_s)$ ……………………………(voltage, spherical aberration)

$\Theta_2 = (\Delta f_M, \Delta f_m, \theta)$ ………………………(maximum defocus, minimum defocus, astigmatism angle)

$\Theta_3 = (C_a, \frac{\Delta V}{V}, \frac{\Delta I}{I}, \alpha, \Delta F, \Delta R)$ …..............(chromatic aberration, electron energy spread,
lens current instability, angular aperture,
vertical sample displacement, in-plane sample displacement)

Defocus vector: $\Delta f(\angle\boldsymbol{\varpi}) = (\Delta f_M\cos(\angle\boldsymbol{\varpi}-\theta), \Delta f_m\sin(\angle\boldsymbol{\varpi}-\theta))$

Envelope: $E(\boldsymbol{\varpi}) = E_{spread}(\boldsymbol{\varpi})E_{coherence}(\boldsymbol{\varpi})E_{drift}(\boldsymbol{\varpi})$

$$E_{spread}(\boldsymbol{\varpi}) = e^{-\frac{\left(\frac{\pi}{4}C_a\lambda\left(\frac{\Delta V}{V}+2\frac{\Delta I}{I}\right)\right)^2}{\log(2)}|\boldsymbol{\varpi}|^4}, E_{coherence}(\boldsymbol{\varpi}) = e^{-\pi^2\alpha^2\left(C_s\lambda^2|\boldsymbol{\varpi}|^3+|\Delta f(\angle\boldsymbol{\varpi})||\boldsymbol{\varpi}|\right)^2}$$

$E_{drift}(\boldsymbol{\varpi}) = J_0\left(\pi\Delta F\lambda|\boldsymbol{\varpi}|^2\right)\mathrm{sinc}\left(|\boldsymbol{\varpi}|\Delta R\right)$ λ : Electron wavelength depending on voltage

Background: $$S_N(\boldsymbol{\varpi}) = b + K_s e^{-|\mathbf{r}_{\Theta_4}(\angle\boldsymbol{\varpi})|\sqrt{|\boldsymbol{\varpi}|}} + K_G e^{-|\mathbf{r}_{\Theta_5}(\angle\boldsymbol{\varpi})|(|\boldsymbol{\varpi}|-|\mathbf{r}_{\Theta 6}(\angle\boldsymbol{\varpi})|)^2} - K_g e^{-|\mathbf{r}_{\Theta_7}(\angle\boldsymbol{\varpi})|(|\boldsymbol{\varpi}|-|\mathbf{r}_{\Theta_8}(\angle\boldsymbol{\varpi})|)^2}$$

$\Theta_i = (R_i, r_i, \beta_i), i = 4,5,\ldots,8$

$\mathbf{r}_{\Theta_i}(\angle\boldsymbol{\varpi}) = (R_i\cos(\angle\boldsymbol{\varpi}-\beta_i), r_i\sin(\angle\boldsymbol{\varpi}-\beta_i))$

Note: Unknown parameters are in red

4. Estimation of the PSD model

Θ_1

↓ Note: Currently estimated parameters are in red

1. Background estimation

↓ $(\Theta_1, b, K_s, K_G, \Theta_4, \Theta_5, \Theta_6)$

2. Envelope estimation

↓ $(\Theta_1, b, K_s, K_G, \Theta_4, \Theta_5, \Theta_6, K, \Theta_3)$

3. Defocus estimation

↓ $(\Theta_1, b, K_s, K_G, \Theta_4, \Theta_5, \Theta_6, K, \Theta_3, \Theta_2)$

4. Parameter refinement

↓ $(\Theta_1, b, K_s, K_G, \Theta_4, \Theta_5, \Theta_6, K, \Theta_3, \Theta_2)$

5. Refinement of parameters estimated in step 4 with additional estimation of K_g,Θ_7, and Θ_8 for a better fit at low frequencies

↓

$(\Theta_1, b, K_s, K_G, \Theta_4, \Theta_5, \Theta_6, K, \Theta_3, \Theta_2, K_g, \Theta_7, \Theta_8)$

Determination of Θ_2 is the most difficult part of the algorithm. Robustness and accuracy of this determination is improved using enhanced PSD in steps 3 and 4. In these steps, the following cost function is optimized:

$$L = \frac{1}{\mathrm{card}\{\Omega\}}\sum_{\boldsymbol{\varpi}_i\in\Omega}\left|PSD'_{experimental}(\boldsymbol{\varpi}_i) - PSD'_{theoretical}(\boldsymbol{\varpi}_i)\right| - \mathrm{w}\rho(PSD'_{enhanced}(\boldsymbol{\varpi}_i), H(\boldsymbol{\varpi}_i))$$

$$PSD'(\boldsymbol{\varpi}) = \frac{PSD(\boldsymbol{\varpi}) - S_N(\boldsymbol{\varpi})}{K^2E^2(\boldsymbol{\varpi})}$$: Normalized PSD

ρ(x,y) : Correlation coefficient between *x* and *y*

w : Weight determining the influence of the PSD enhancement term on the optimization algorithm (w>0)

Ω : Annular mask in the frequency domain

5. Results of PSD estimation on a single micrograph

Switching off the term based on the enhanced PSD (w=0):

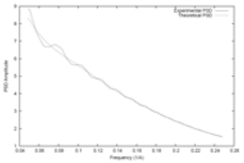

Radial averages of experimental and estimated PSDs. The estimated PSD does not fit well the experimental PSD since the algorithm fails to estimate Θ_2 accurately.

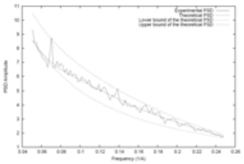

Sample profiles of experimental and estimated PSDs. The envelope and the background determine an upper bound and an lower bound for the PSD, respectively.

Switching on the term based on the enhanced PSD (w=5):

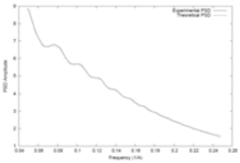

Radial averages of experimental and estimated PSDs. The estimated PSD fits much better the experimental PSD than in case w=0 (estimation of Θ_2 is more accurate).

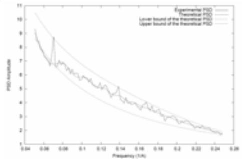

Sample profiles of experimental and estimated PSDs. The envelope and the background determine an upper bound and an lower bound for the PSD, respectively.

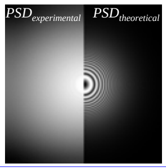

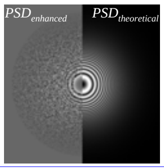

Literature

[1] Jonic, S., Sorzano, C.O., Cottevieille, M., Larquet, E. and Boisset, N., 2007. A novel method for improvement of visualization of power spectra for sorting cryo-electron micrographs and their local areas. J Struct Biol, 157(1): 156-67.

[2] Velazquez-Muriel, J.A., Sorzano, C.O., Fernandez, J.J. and Carazo, J.M., 2003. A method for estimating the CTF in electron microscopy based on ARMA models and parameter adjustment. Ultramicroscopy, 96(1): 17-35.